



High Deposition Rate Symmetric Magnet Pack for High Power Pulsed Magnetron Sputtering



Priya Raman ^{a,*}, Ivan Shchelkanov ^{a,b}, Jake McLain ^a, Matthew Cheng ^a, David Ruzic ^a, Ian Haehnlein ^{a,c}, Brian Jurczyk ^c, Robert Stubbers ^c, Sean Armstrong ^d

^a University of Illinois at Urbana Champaign, IL, USA

^b National Nuclear Research University (MEPhI), Moscow, Russian Federation

^c Starfire Industries, IL, USA

^d Kurt J. Lesker Company, PA, USA

ARTICLE INFO

Article history:

Received 1 July 2015

Revised 25 November 2015

Accepted in revised form 21 December 2015

Available online 22 December 2015

Keywords:

HPPMS

HiPIMS

HiPIMS deposition rates

Magnetron sputtering

HiPIMS power supply

High deposition rate magnet pack for HPPMS

ABSTRACT

High power pulsed magnetron sputtering is a promising physical vapor deposition technique with two minor challenges that obstruct its broader implementation in industry and its use by researchers. The first challenge is the availability of low cost HPPMS power supplies with output power under 2 kW. Such power supplies are suited for circular planar magnetrons with target diameters between 50 mm to 150 mm. The second challenge is the overall lower deposition rates of HPPMS when compared with direct current magnetron discharges. The “ε” magnet pack designed for a 100 mm sputter magnetron which was developed by the Center for Plasma Material Interactions at the University of Illinois at Urbana Champaign in collaboration with Kurt J. Lesker Company was capable of producing twice higher deposition rates in HPPMS compared to a conventional magnet pack. The cylindrically symmetric “TriPack” magnet pack presented here was developed based on magnetic field design solutions from the “ε” magnet pack in order to keep the high deposition rates, but improve deposition uniformity, without the need for substrate rotation. The new cylindrically symmetric magnet pack for 100 mm diameter targets, along with a specially designed cooling well provides stable operation at 2 kW average power, even with low-temperature melting-point target materials. The deposition rates from the TriPack magnet pack is compared with a commercial conventional magnet pack for DC and HPPMS power supplies.

© 2015 Elsevier B.V. All rights reserved.

1. Introduction

High power pulsed magnetron sputtering (HPPMS), or high power impulse magnetron sputtering (HiPIMS), is a type of magnetron sputtering technique where high power pulses, with durations of hundreds of microseconds are applied to the magnetron target at frequencies ranging from a few Hz to several kHz. In such a discharge, the peak power densities during the pulse can be on the order of several tens of kilowatts per square inch whereas the average power densities are comparable to or equal to direct current magnetron sputtering (dcMS) discharges [1] to avoid melting or overheating the sputtering target. These high peak power pulses result in electron densities of 10^{19} m^{-3} , which are three orders of magnitude higher than dcMS discharges [2]. Such high electron densities lead to ionization of the sputtered material, which in turn leads to a higher density of ion flux towards the substrate [3]. The higher ionization fraction of sputtered material, and the lower thermal load on to the substrate lead to high

quality thin films [4,5]. Until recently, it was believed that HPPMS/HiPIMS was a technique with low deposition rates that could only be used in a limited number of applications [6]. To understand the reasons behind such low deposition rates in HiPIMS, extensive studies were performed by many research teams around the globe [7]. The importance of the following aspects of a magnetron were shown: magnetic field magnitude and the magnetic field profile on the magnetron target surface [8–10], plasma impedance [11], plasma instabilities [12] and power supply pulsing parameters [13,14].

The wide range of mentioned experimental work was not enough to develop a mathematical model that could describe the quantitative contributions from each of the above mentioned factors to deposition rates in HiPIMS. A quick conclusion from all the previous experimental work is that, the shape and magnitude of the magnetic field above the cathode has the major contribution to the deposition rates. The Center for Plasma Material Interactions (CPMI) started out with a series of experiments [15] to search for an optimal magnetic field configuration for pulsed magnetron discharges. The experimental results for a 4” diameter magnetron sputter gun are discussed in this article.

* Corresponding author.

2. Experimental set-up

Sputtering high-purity atomic deposition experiment (SHADE) is a dual magnetron setup for depositing thin films in an ultra-high vacuum (UHV) environment. The SHADE chamber (Fig. 1(a)) has a load lock for sample transfer and a rotatable substrate holder for increasing the film uniformity during deposition. Huettinger TruPlasma Highpulse 4002 DC Generator power supply (average power: 0–10 kW; maximum voltage: 2000 V; maximum current: 1000 A; pulse length 1–200 μ s; frequency: 1–400 Hz) and Starfire impulse power supply (average power: 0–2 kW; maximum voltage: 1000 V; maximum current: 200 A; pulse length 5 μ s–1 ms; frequency: 1 Hz–10 kHz) were used for HiPIMS discharges. The Advanced Energy pinnacle plus power supply (average power: 0–10 kW; voltage: 325–650 V; maximum current: 30 A) was used for dcMS discharges. Aluminium, titanium, copper and carbon targets were tested in this work. The deposition rates were measured using a dual water-cooled Quartz Crystal Microbalance (QCM) that was placed 4" from the target surface, on the axis of the magnetron gun. The QCM assembly was attached to a rotatable feed through. During the experiments, the QCM assembly was moved from the center of one magnetron to the other so the deposition rate comparison experiments could be done without breaking the vacuum. The base pressures on the SHADE chamber were $\sim 1 \times 10^{-7}$ Torr and the gas flow to the chamber was regulated by mass flow controllers (MFC). Kurt J. Lesker Company's standard 4" Torus magnetron sputter gun was used for this work. The commercial Torus comes with a conventional arch

shaped magnetic field configuration (Fig. 2(a), (d) and (g)), where the arch of the magnetic field lines starts from the center of the magnetron target and continues to the outer edge. This type of magnet pack will be referred to as a "conventional magnet pack". For the TriPack that is described in this article, a specially designed magnetron and target were used. The target was 0.25" thick and was machined to accommodate four concentric rings made out of magnetic material (soft iron). These rings served as magnetic field conduits that helped in obtaining the same magnetic field values above the target as in the conventional pack. Since these rings were only 0.125" tall and were embedded in to the back of the target surface that is attached to the cooling well side, no iron was exposed to plasma. Also, the target was machined to look like a pre-eroded target to obtain the required magnetic field magnitudes on the target surface. Fig. 1(b) is a 2D axisymmetric illustration of the modified TriPack target, where the gray colored rectangles represent the iron pieces. The colored iso-lines show the total magnitude of the magnetic field in Gauss. This should not be misinterpreted with the surface magnetic field plots shown in Fig. 2(a)–(c) where only the radial component of magnetic field is presented.

3. Magnet field design and simulations

COMSOL Multiphysics finite element analysis software was used to simulate the magnetic field profile above the target surface in this work. The magnetic and electric field modules of COMSOL Multiphysics was used to calculate the magnetic flux densities and surface magnetic

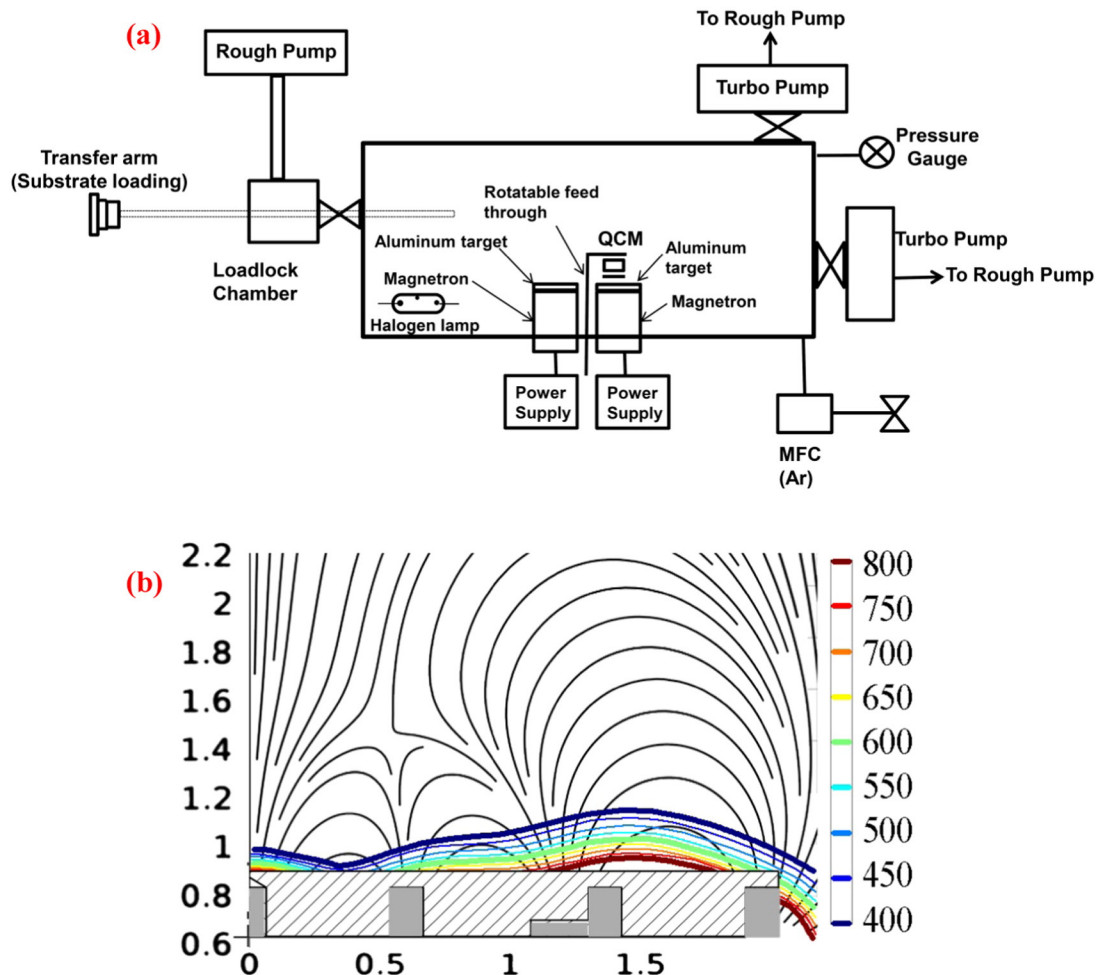


Fig. 1. (a) Schematic diagram of the SHADE chamber, (b) 2D axisymmetric illustration of the modified TriPack target. The colored iso-lines show the total magnitude of magnetic field in Gauss.

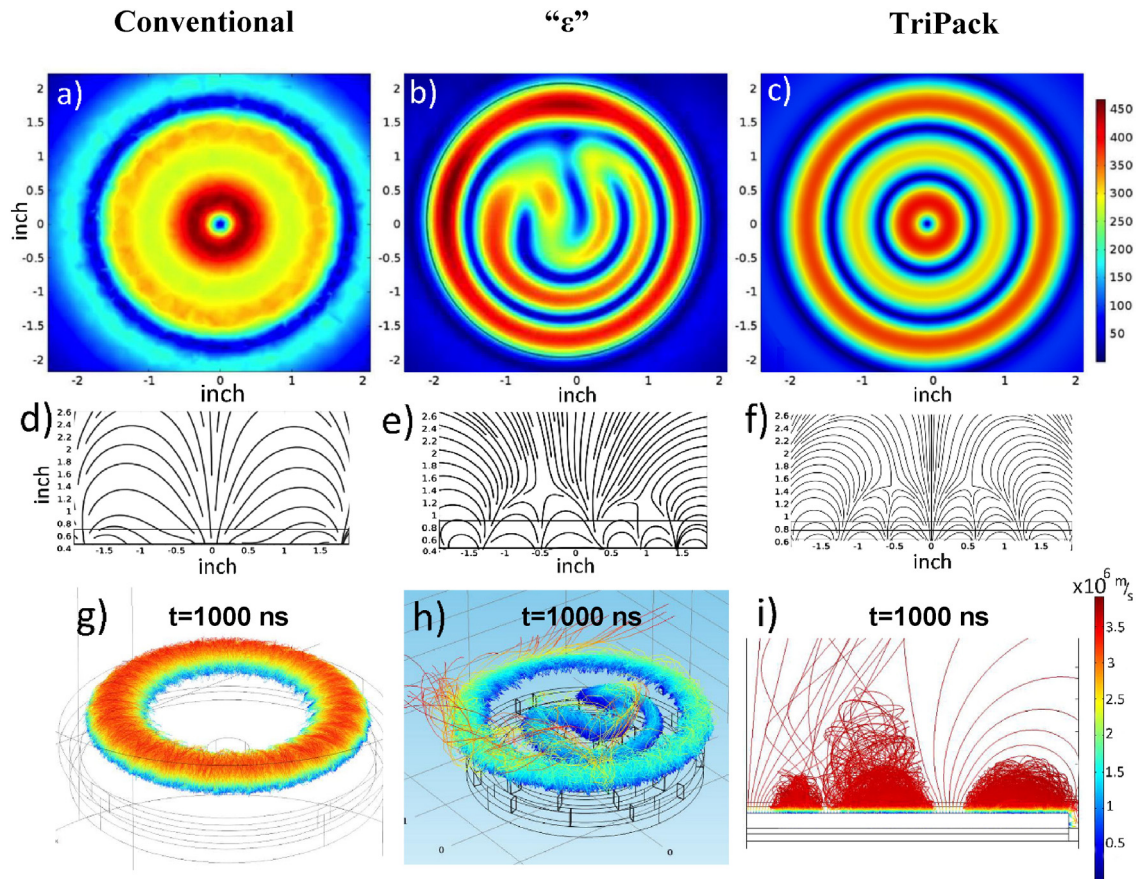


Fig. 2. (a) $B_{//}$ on the target surface of the conventional magnet pack, (b) $B_{//}$ on the target surface of the “ ϵ ” magnet pack, and (c) $B_{//}$ on the target surface of the TriPack. (d) Streamline plot of B_x and B_y components in the conventional magnet pack. (e) Streamline plot of B_x and B_y components in the “ ϵ ” magnet pack. (f) Streamline plot of B_x and B_y components for the TriPack. (g) 3D Electron trajectory from the conventional magnet pack. (h) 3D Electron trajectory from the “ ϵ ” magnet pack. (i) 2D axisymmetric Electron trajectory from the TriPack.

field, $B_{//}$ ($\sqrt{B_x^2 + B_y^2}$, XY plane is parallel to the target surface) for a given arrangement of magnets. The distribution of $B_{//}$ above the target surface helps in predicting the racetrack region corresponding to a certain arrangement of magnets in a magnet pack. All models have one-to-one scale. The charged particle tracing (CPT) module of COMSOL Multiphysics was used to simulate the electron trajectories above the target surface for different magnet packs. In the CPT module, the electrons were injected into the race-track from the target surface with an energy of 0.1 eV. These electron trajectory simulations take into account electron–electron coulombic interactions and the electron–field interactions that arise from the static electric and magnetic fields. This approach allows predicting the general behaviour of electrons in the trap. The authors would like to point out that this approach is a crude method for a HiPIMS discharge but still gives some information on electron trajectories.

The electron trajectories, magnetic fields, and electric fields were simulated inside a sphere of 25 in. diameter to avoid edge effects on boundaries in the model. The outer wall (the edge of the whole model) boundary condition for magnetic field was set to zero surface currents and also zero potential for electric field simulations. The magnets were modeled as recommended by the COMSOL software manual. In the model, the cathode was biased to -600 V and the plasma sheath was artificially set to 1 mm. In this artificial sheath region on the top of the target surface, 85% of the voltage was dropped so it mimics a more realistic sheath drop. The time step for the model was controlled by the COMSOL solver and was as small as 0.01 ns. All electrons were released homogeneously from cathode surface at time step zero. In order to obtain more data points for trajectory tracing, the total number of electrons released from the target surface was set to 1000.

Fig. 2(a)–(f) shows the modeling results for the conventional pack, “ ϵ ” magnet pack, and the “TriPack”. The performance of “ ϵ ” magnet pack and its comparison to the conventional magnet pack design are discussed in detail in the work published by Raman et al. [16]. Fig. 2(g) shows the 3D electron trajectory in the conventional magnet pack. It can be observed that the electrons are well confined and recycled in this magnet pack.

The 3D electron trajectory in the “ ϵ ” pack (Fig. 2(h)) shows that there is electron confinement as well as some electron loss. The electron loss is due to the existence of open field lines in the “ ϵ ” pack. The electrons follow the open field lines and therefore ions follow the electrons due to ambipolar diffusion. This helps to achieve higher ionized deposition flux on to the substrate.

Fig. 2(i) shows the 2D axisymmetric view of the electron trajectories in the TriPack. It can be observed that the central region has electrons escaping from the arc trajectory, this could be the reason for the increased deposition rates, which is discussed in the following section. Although this assumption of the particle escape path seems to be the most probable one, the plasma dynamics in such a sophisticated magnetic configuration like the TriPack’s, can involve other effects, which could contribute to the increase in deposition rates.

4. Experimental results and discussion

The new design of the magnetic field implemented in the TriPack provides stable magnetron discharge ignition and operation at pressures greater than 1 mTorr. The HiPIMS discharge volt–ampere (V–I) characteristic for the TriPack follows the conventional magnetron trend which is $V \propto I^n$ where, “n” is the performance index of the electron

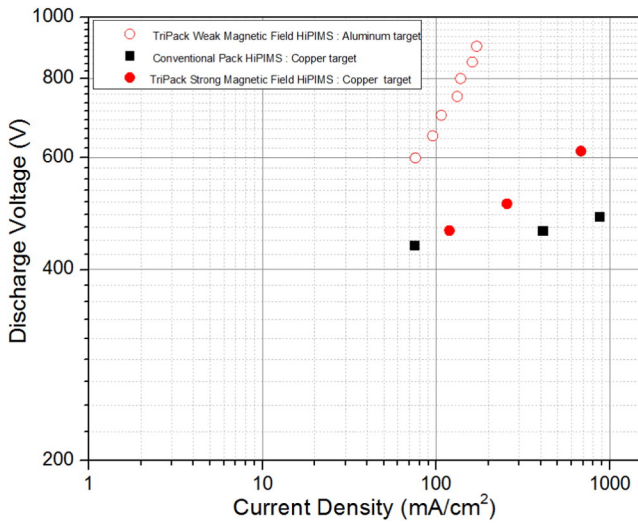


Fig. 3. Volt-ampere characteristics of the conventional pack and TriPack.

trap [17], V is the discharge voltage and I is the peak current during a discharge pulse. The X axis on Fig. 3 represents the current density, which is the single pulse peak current divided by the target erosion area, and the Y axis represent the discharge voltage. This plot was constructed from the voltage and current traces obtained from the Huettinger power supply on a copper target, at 10 mTorr argon pressure. It can be observed from Fig. 3 that the HiPIMS discharge for the TriPack has a similar V-I trend to the conventional pack discharge, as described by Thornton et al. [17]. Hollow red color legends correspond to the Tri-Pack for an aluminium target with weaker magnetic fields. The weaker fields were obtained by removing magnetic rings from the target. The magnetic field was reduced by more than 200 G when the magnetic rings were removed, but the shape of magnetic field lines remained the same. This was confirmed from modeling in COMSOL.

The performance of the TriPack was also tested using Starfire impulse HiPIMS power supply. This power supply provides more “freedom” for parameter optimization during HiPIMS discharges. Its operation frequency ranges from 1 Hz to 10 kHz, can reach pulse lengths up to 1 ms, and can provide up to 2 kW average power, which is more than enough to sustain HiPIMS discharges on smaller magnetrons. Panels (a) and (b) in Fig. 4 are the voltage and current traces obtained from the conventional and TriPack, respectively using the Starfire impulse power supply for an aluminium target at 13 mTorr and an average power of 500 W. In the case of conventional HiPIMS operation, the

current slowly reaches 150 A (Fig. 4(a)) at the end of the pulse for pulsing parameters of 850 V (discharge voltage), 220 Hz (frequency) and 30 μ s pulse (pulse time). The current in the TriPack steeply increases to only about 12 A for pulsing parameters of 850 V, 300 Hz and pulse time of 200 μ s. There is a distinct difference in the shape of the discharge current trace between both the magnet packs. Such a dramatic difference can be attributed to a difference in the plasma dynamics between in this new magnetic field profile and conventional magnetic field profile.

The most dramatic difference is seen in the peak discharge currents. Although the TriPack peak current is only 12 A, the peak electron density and temperature were measured to be $1-6 \times 10^{18}/\text{m}^3$ and $4 (\pm 3)$ eV respectively at 1" away from the titanium target surface. The electron temperatures and densities were measured using a Triple Langmuir Probe (TLP) technique and these electron densities and temperatures are typical for HiPIMS discharge.

The next, and most appealing, difference between the TriPack and conventional magnet pack is the deposition rates. The deposition rates from the conventional pack and TriPack were obtained at 13 mTorr and 500 W average power with Advanced Energy DC, Huettinger HiPIMS and Starfire IMPULSE HiPIMS power supplies. The pulsing parameters (discharge voltage, pulse time and frequency) were different for different target materials, magnet packs and HiPIMS power supplies (Huettinger and Starfire impulse) but, the average power was always kept at 500 W. Three different target materials, namely titanium, carbon and aluminium, were compared for deposition rates. The results from the deposition rate experiments are summarized in Fig. 5.

The Y axis in Fig. 5 represents the deposition rates normalized to conventional pack DC deposition rates at 500 W for each material, and the X axis represents the different target materials. In the case of titanium, TriPack HiPIMS deposition rates were higher than the conventional pack DC deposition rates. Titanium deposition rate measurement can be difficult because the titanium targets can get hot during long term operation. There are several publications [18] that comment about this effect. The deposition rate experiments from the conventional and Tri-Pack magnet packs were performed with a cold titanium target to avoid all hot target effects. In order to operate with the cold titanium target, the deposition rate measurements were done for only 15 s with a cooling time of about 30 s between measurements. A series of deposition rate measurements were done for 15 s and compared to the average deposition rate over several experiments. The deposition rates remained the same for all the experiments. With carbon target, the TriPack HiPIMS deposition rates were about the same as the conventional DC deposition rates and in the case of an aluminium target, TriPack HiPIMS deposition rates were lower than conventional DC deposition rates but higher than conventional HiPIMS deposition rates.

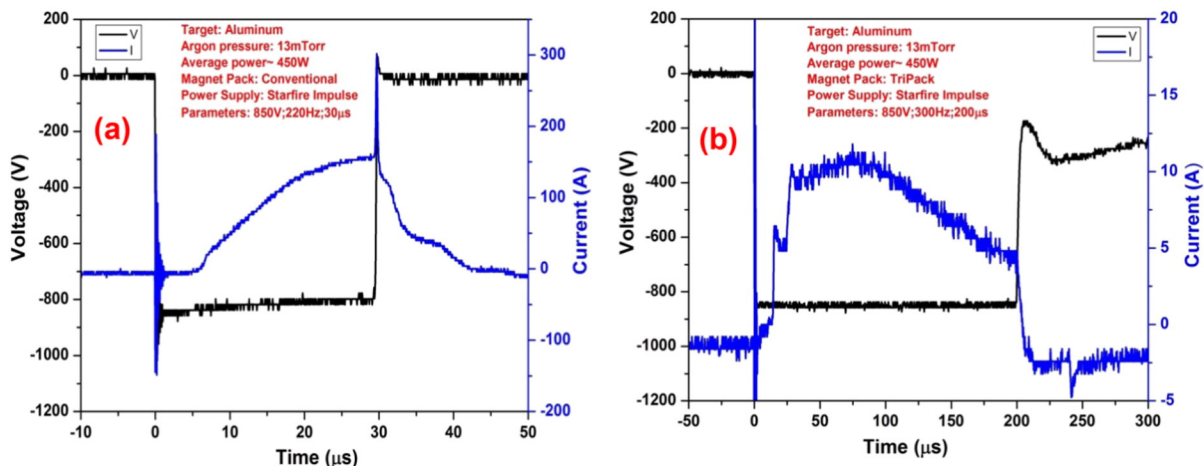


Fig. 4. (a) Voltage and current traces from Starfire impulse power supply for conventional pack. (b) Voltage and current traces from Starfire impulse power supply for TriPack.

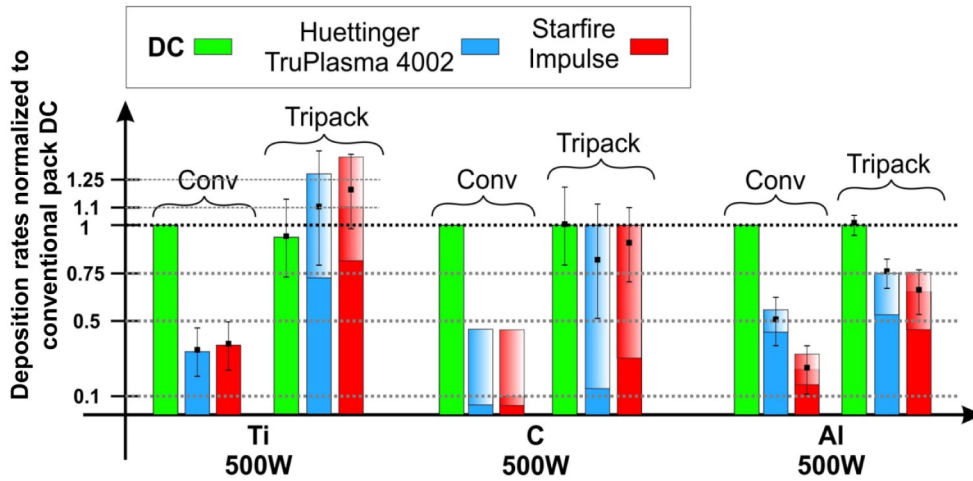


Fig. 5. Deposition rates from conventional pack and the TriPack with titanium, carbon and aluminium targets at 13 mTorr normalized to the DC deposition rates with the conventional pack. All deposition rates on titanium were measured from a “cold” titanium target. The gradients on the bar plot represent the range of deposition rates that can be obtained by varying pulsing parameters, but keeping the average power at 500 W. The black error bars represent the error in acquiring the QCM data during our experiments. DC deposition rates with the conventional pack were ~1 Å/s for titanium, ~0.1 Å/s for carbon and ~12 Å/s for aluminium at 4” away from the target.

The effects of changing pulsing parameters in HiPIMS are more distinct in the TriPack than in conventional pack. In Fig. 5, the color gradient represents the magnitude of the deposition rate variation as a function of varying pulsing parameters. It should be noted that titanium and carbon are very sensitive to pulsing parameters. Here we do not show all parameters, as it is a subject of another article, but the influence of pulsing parameters on the deposition rates of copper target are presented in Fig. 6. Copper was chosen because it gives the highest deposition rates in comparison with most other materials, and does not have the “hot target” problem seen with titanium targets.

The data presented in Fig. 6 makes it clear that HiPIMS discharge physics is very sophisticated. The deposition rate increased twofold simply by increasing the pulse time by a factor of 2 and decreasing the pulsing frequency, while the discharge voltage was kept constant. The pure argon pressure during these experiments was kept at 10 mTorr. It should be noted that the deposition rates around 500 W were taken exactly at 500 W as expressed in Fig. 6. The data points have an offset on the power axis to display the error bars more clearly. The lowest

deposition rates were observed with a low repetition rate and longer pulses, and with high repetition rates and very short pulses.

The reason for the observed change in the deposition rates when applying different pulsing parameters at the same average power may be due to the change in the local gas density during the discharge, but more detailed work is needed to develop a phenomenological explanation for these experimental results. The deposition rates did not change with the change in pulsing parameters for the conventional pack HiPIMS case, which clearly indicates that this pulsing effect on deposition rates is due to the unique TriPack magnetic field configuration.

There have been several publications in the past that show that lowering the magnetic field strength leads to higher deposition rates, due to reduction in the metal ion “return effect” [19]. This is not the case for the TriPack, as the radial component of the magnetic field on the surface of the target is the same as the conventional pack, which can be seen in Fig. 7. A careful material flux model is required to explain in detail the increase in deposition rate in the TriPack. This is because the race track area of the conventional pack is only 6 in.², whereas the race track area of the TriPack is ~8 in.². The TriPack race track area is 25% larger, but has much lower discharge current when compared

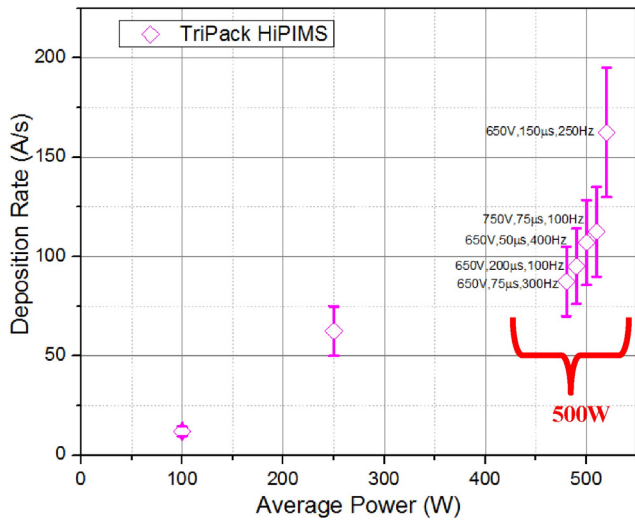


Fig. 6. Variation of copper HiPIMS deposition rates by pulsing parameters change in TriPack at 10 mTorr. The presented deposition rates around 500 W were taken exactly at 500 W but the data points have been offset on the power axis to display the error bars more clearly.

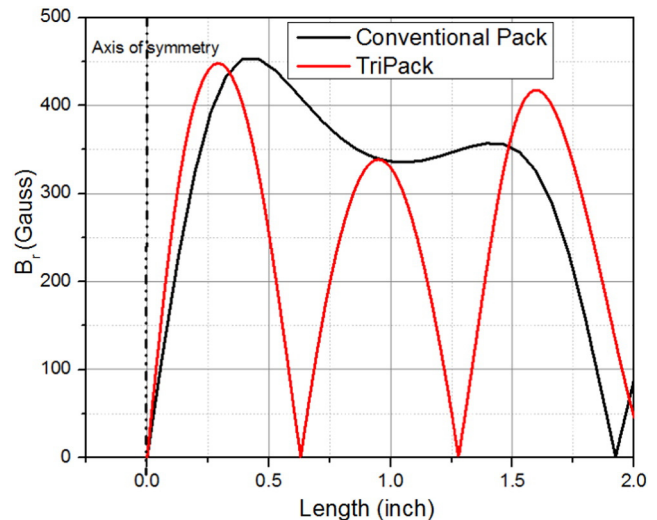


Fig. 7. Comparison of |Br| from conventional and TriPack on target surface in 2D axisymmetric view.

with the conventional pack. Both these observations combined do not support the simple explanation that higher race-track area gives higher deposition rates.

5. Conclusion

The new cylindrically symmetric TriPack provides higher deposition rates in HPPMS discharges. Unlike DC power supply, with HPPMS power supplies, the deposition rates in the TriPack could be varied by a factor of 2 simply by changing the pulsing parameters while keeping the average power constant. TriPack's higher deposition rates in HPPMS and their variation with pulsing parameters originate from the magnetic field topology, which in turn dictates the plasma dynamics that is very different when compared to the plasma dynamics of the conventional magnet pack. Understanding of the plasma dynamics in the TriPack and conventional pack will require more rigorous experimental and modeling efforts.

Acknowledgments

This research was funded by the NSF Center for Lasers and Plasmas for Advanced Manufacturing under the I/UCRC program grant number 15-40030. This work was carried out in part in the Frederick Seitz Materials Research Laboratory Central Research Facilities and Visualization Laboratory at Beckman Institute in University of Illinois.

References

- [1] D. Lundin, K. Sarakinos, An introduction to thin film processing using high-power impulse magnetron sputtering, *J. Mater. Res.* 27 (05) (2012) 780–792.
- [2] J. Alami, et al., Plasma dynamics in a highly ionized pulsed magnetron discharge, *Plasma Sources Sci. Technol.* 14 (3) (2005) 525.
- [3] G. Greczynski, L. Hultman, Time and energy resolved ion mass spectroscopy studies of the ion flux during high power pulsed magnetron sputtering of Cr in Ar and Ar/N₂ atmospheres, *Vacuum* 84 (9) (2010) 1159–1170.
- [4] W. Münz, et al., Industrial applications of HIPIMS, *Journal of Physics: Conference Series*, IOP Publishing, 2008.
- [5] A.P. Ehiasarian, High-power impulse magnetron sputtering and its applications, *Pure Appl. Chem.* 82 (6) (2010) 1247–1258.
- [6] M. Samuelsson, et al., On the film density using high power impulse magnetron sputtering, *Surf. Coat. Technol.* 205 (2) (2010) 591–596.
- [7] A. Anders, Deposition rates of high power impulse magnetron sputtering: physics and economics, *J. Vac. Sci. Technol. A* 28 (4) (2010) 783–790.
- [8] J. Bohlmark, et al., Guiding the deposition flux in an ionized magnetron discharge, *Thin Solid Films* 515 (4) (2006) 1928–1931.
- [9] L. Meng, et al., Downstream plasma transport and metal ionization in a high-powered pulsed-plasma magnetron, *J. Appl. Phys.* 115 (22) (2014), 223301.
- [10] A. Ehiasarian, A. Vetushka, Magnetron configuration to enhance deposition rate in high power impulse magnetron sputtering, SVC, Society of Vacuum Coaters—52nd Annual Technical Conference, May 9–14, 2009.
- [11] F. Papa, et al., Deposition rate characteristics for steady state high power impulse magnetron sputtering (HIPIMS) discharges generated with a modulated pulsed power (MPP) generator, *Thin Solid Films* 520 (5) (2011) 1559–1563.
- [12] D. Lundin, et al., Cross-field ion transport during high power impulse magnetron sputtering, *Plasma Sources Sci. Technol.* 17 (3) (2008), 035021.
- [13] S. Konstantinidis, et al., Influence of pulse duration on the plasma characteristics in high-power pulsed magnetron discharges, *J. Appl. Phys.* 99 (1) (2006), 013307.
- [14] G. West, et al., Measurements of deposition rate and substrate heating in a hipims discharge, *Plasma Process. Polym.* 6 (S1) (2009) S543–S547.
- [15] H. Yu, et al., Investigation and optimization of the magnetic field configuration in high-power impulse magnetron sputtering, *Plasma Sources Sci. Technol.* 22 (4) (2013), 045012.
- [16] P. Raman, et al., High power pulsed magnetron sputtering: a method to increase deposition rate, *J. Vac. Sci. Technol. A* 33 (3) (2015), 031304.
- [17] J.A. Thornton, Magnetron sputtering: basic physics and application to cylindrical magnetrons, *J. Vac. Sci. Technol.* 15 (2) (1978) 171–177.
- [18] J. Tesař, J. Martan, J. Rezek, On surface temperatures during high power pulsed magnetron sputtering using a hot target, *Surf. Coat. Technol.* 206 (6) (2011) 1155–1159.
- [19] A. Mishra, P. Kelly, J. Bradley, The evolution of the plasma potential in a HiPIMS discharge and its relationship to deposition rate, *Plasma Sources Sci. Technol.* 19 (4) (2010), 045014.